



ChemComm

Rational design and synthesis of yellow-light emitting triazole fluorophores with AIE and mechanochromic properties

Journal:	<i>ChemComm</i>
Manuscript ID	CC-COM-01-2019-000262.R1
Article Type:	Communication

SCHOLARONE™
Manuscripts

Rational design and synthesis of yellow-light emitting triazole fluorophores with AIE and mechanochromic properties

Qi Lai,^a Qing Liu,^a Kai Zhao,^a Chuan Shan,^b Lukasz Wojtas,^b Qingchuan Zheng,^c Xiaodong Shi,^{*a,b} Zhiguang Song^{*a}

Received 00th January 20xx,
Accepted 00th January 20xx

DOI: 10.1039/x0xx00000x

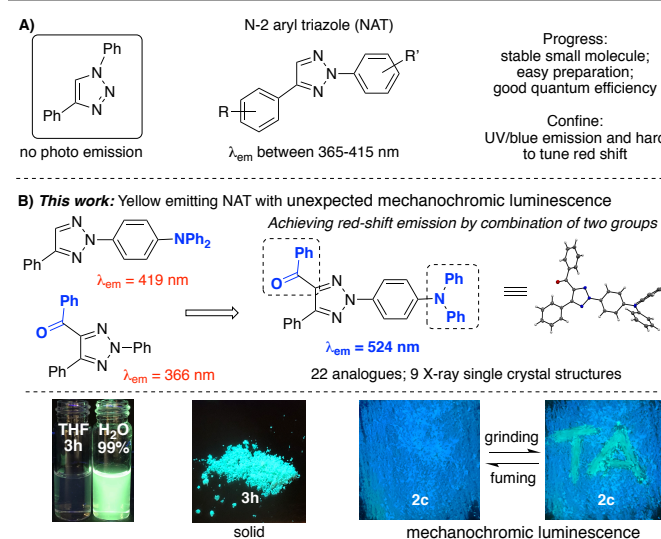
www.rsc.org/

Previously, we reported N-2-aryl triazoles (NAT) exhibited good fluorescent activity in UV/blue light range. In the effort to achieve biocompetitive NAT fluorophores with green/yellow emission, a new class of 4-keto-2-(4'-N,N-dipheyl)-phenyl triazoles were designed and synthesized. Herein, we present our study of these novel fluorophores which demonstrated excellent luminescent emission both in solution (Φ up to 96%) and in solid state (Φ up to 43%). Furthermore, these new compounds showed aggregation-induced emission (AIE) properties as well as reversible mechanochromic luminescence properties, which suggested their potential applications in chemical and material science.

Fluorescence active small organic molecules are important class of compounds in chemical¹, biological² and material³ research. In general, many factors including high luminescence efficiency, high thermal stability, good accessibility and easy modification are assessed for organic phosphor's applications.⁴

In the past decade, our efforts on triazole derivative synthesis⁵ have led to the discovery of N-2-aryl-1,2,3-triazoles as good fluorescence emission compounds, while the N-1 isomers (1,4-disubstituted-triazole) showed almost no emission.⁶ As shown in **Scheme 1A**, changing different aryl substitutions on both N-2 and C-4 position can only cause a small emission wavelength shift. Although fluorophores with UV/blue light emission are important for certain applications⁷, those with emission at lower energy (green/yellow/red light region) is preferred for applications in biological systems.⁸ Herein, we have devoted many efforts to developing NAT-derivatives with longer emission wavelength. By simultaneously incorporating electron-rich substitutions on the N-2 phenyl

position and electron-deficient substitutions on the C-4 position, a series of yellow emitting NAT fluorophores (λ_{em} up to 550 nm) with high quantum yields both in solution and in solid state were obtained. Moreover, these compounds showed aggregation induced emission (AIE) properties and interesting mechanochromic luminescence, suggesting a promising strategy to construct solid fluorophores from simple 1,2,3-triazole derivatives (**Scheme 1B**).



Scheme 1. Developing yellow emitting NAT fluorophores.

As a general design principle, extending conjugation system of the fluorophore will lead to red-shift of the emission wavelength due to the reduced energy gap between its highest occupied molecular orbital (HOMO) and the lowest unoccupied molecular orbital (LUMO).⁹ Considering that 1,2,3-triazole is a highly electron deficient functional group, incorporation of electron-donating groups (EDG) should bring the emission to red-shift. However, even with strong EDG like N, N-dimethyl (**1c**), limited red-shift was observed with λ_{em} at 427 nm. (**Figure 1A**, see detailed syntheses of all compounds and their optical dates in SI). Notably, 1,2,3-triazole is a very stable aromatic

^a State key Laboratory of Supramolecular Structure and Materials, College of Chemistry, Jilin University, Changchun, Jilin 13002 China; E-mail: szq@jlu.edu.cn

^b University of South Florida, Tampa, FL 33620, USA. E-mail: xmshi@usf.edu

^c International Joint Research Laboratory of Nano-Micro Architecture Chemistry, Institute of Theoretical Chemistry, Jilin University, Changchun 130023, P. R. China.

† Electronic Supplementary Information (ESI) available. For ESI and crystallographic data in CIF or other electronic format see DOI: See DOI: 10.1039/x0xx00000x

structure. Thus, it often forms poor conjugation between N-2 aryl due to energy penalty for breaking aromaticity. As a result, EDG substituted NAT at best could only form resonance structure **A**, bearing triazole (TA) stabilized anion, which leads to the limited emission change.

(A) Limited impact of EDG on N-2-aryl group

	$\lambda_{\text{excitation}}$ (nm)	$\lambda_{\text{emission}}$ (nm)	Stokes shift (nm)	Φ (%)
1a , R=H; 1b , R=OMe; 1c , R=NMe ₂ ; 1d , R=NPh ₂	295	351	65	98
	305	374	69	96
	316	427	111	93
	348	419	71	78

(B) Hypothesis: extending electron conjugation with the combination EDG and EWG

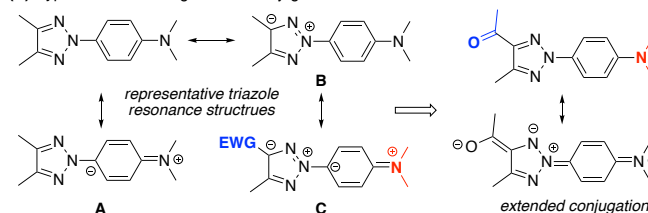


Figure 1. General strategy to achieve NAT red-shift.

To access extended conjugation, an accessible TA resonance structure **B** is necessary, which requires the overall electron density delocalized from the three adjacent nitrogens to the carbon. With this consideration in mind, we postulated that introducing electron withdrawing group (EWG) on triazole carbon with help the electron delocalization, favoring the resonance structure **B**. Thus, we proposed that the combination of EDG on N-2 aryl and EWG on carbon will build the extended conjugation, giving the desired red-shift NAT as shown in intermediate **C** (Figure 1B). To verify this hypothesis, we prepared triazole analogues **2a-2d** with varied EWGs on triazole C-4 position. Their PL data are summarized in Figure 2.

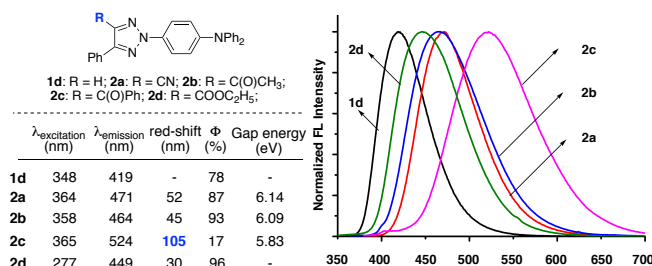


Figure 2. Significant red-shift with EDG/EWG substituted TPA-NAT.

As proposed, introducing EWG (cyan or carbonyl group) on C-4 position gave the expected red-shift while maintaining excellent fluorescence emission. Notably, with 4-phenylcarbonyl substitution (**2c**), a very dramatic red-shift (105 nm) was observed. Compared with blue-emitting compounds **2a** and **2b**, quantum yield for **2c** was lower, which is common for long wavelength emission fluorophore. Density functional theory (DFT) calculations based on single crystal structures were also conducted (Table S13). Compared with **2a/2b**, **2c** possesses a smaller energy gap (5.83 eV), thus giving a longer wavelength of fluorescence emission. Encouraged by this result, a series of EDG/EWG modified NAT compounds were prepared and their optical properties in THF solution are summarized in Table 1.

Table 1. Optical properties of EDG/EWG modified NAT compounds in THF solution^[a]

Comp	λ_{exc} (nm)	λ_{em} (nm)	Life time τ_{avg} (ns)	Φ (%)	Comp	λ_{exc} (nm)	λ_{em} (nm)	Life time τ_{avg} (ns)	Φ (%)
3a	330	366	3.099	0.37	3h	368	470	3.199	0.18
3b	297	377	-	0.62	3i	364	537	2.116	18
3c	335	550	6.309	4.1	3j	369	533	1.464	52
3d	341	473	1.707	1.3	3k	368	530	2.556	36
3e	365	524	3.182	25	3l	362	537	1.918	4.3
3f	357	540	2.224	12	3m	369	520	3.494	5.7
3g	365	542	1.576	11	3n	370	505	1.467	7.8

^[a]Fluorescence emission of compound **3a-3l**. Concentration: 20 $\mu\text{mol/L}$ in THF.

First, for all the C-4 phenylcarbonyl substituted triazole (**3b-3d**), EDGs at N-2 aryl gave rise to the obvious redshift. Interestingly, structurally rigid carbazole substituted NAT **3d** gave less red-shift, which was likely caused by the poor conjugation between nitrogen and N-2 phenyl due to their steric repulsion. Evaluation of the arylcarbonyl group on C-4 position confirmed that electron deficient aryl substituents could enhance the overall emission. NATs with 4-F, 4-Br and 4-Cl benzene and naphthyl substitution all resulted in red-shifts with strong emission. In contrast, the penta-fluoro benzene substituted NAT **3h** gave less red-shift ($\lambda_{\text{max}}=470$ nm) and very low quantum yield in solution. This can be explained by the strong electronic repulsion between F and triazole N, which were confirmed by the crystal structures showing longer distance between F-N (2.908 Å) in **3h** over the H-N distance (2.760 Å) in **3e**. (see crystal structures in Figure S85). Similarly, the 2-fluoro phenyl and 2,6-difluoro phenyl substitution NAT **3m** and **3n** also exhibited low fluorescence quantum yield in solution, which further supported the above conclusion.

In addition, different substituents on triazole C-5 position were evaluated. Besides phenyl (**2c**), NATs with other functional groups were prepared, including trimethylsilyl (**3j**), hydrogen (**3k**) and electron-donating 4-(N,N-diphenyl)phenyl (**3l**). Although red-shift caused by C-5 substitution with either trimethylsilyl or hydrogen was trivial (about 10 nm), the overall emissions remained in the green-yellow light region. Importantly, significant enhancement of emission quantum yields was achieved, which was likely caused by the improved conjugation with less steric hindrance on C-5 position. Interestingly, incorporation of another EDG on the C-5 position **3l** did not result in efficient emission, which might be ascribed for the lack of effective electronic conjugations. Therefore, by screening NAT of various substitutions, we developed an effective strategy to achieve NAT green/yellow fluorophore *via* tuning the combination of EDG/EWG on NAT.

As motioned above, while electron deficient arylcarbonyl NATs (such as **3f-3g**) generally gave red-shift emissions with high efficiency, it is worth noticing that the pentafluorophenyl substituted NAT **3h** resulted in poor emission with quantum yield <1%. To understand the cause of these results, single crystal structures of nine NATs have been successfully obtained (see details in Figure S78-86). Structures of compounds **2c** and **3h** are shown in Figure 3. For compound **2c**, the dihedral angle between triazole and carbonyl (C=O) is 37.2° and TA vs Ph is

54.1°, not even close to coplanar conformation. Moreover, while compounds **2c** and **3h** clearly gave different PL property in solution, the solid-state X-ray crystals showed very similar geometry. Their twisted conformation aroused our interest to know whether this type of NAT would show different luminescence properties in solid state and exhibit aggregation-induced emission (AIE).

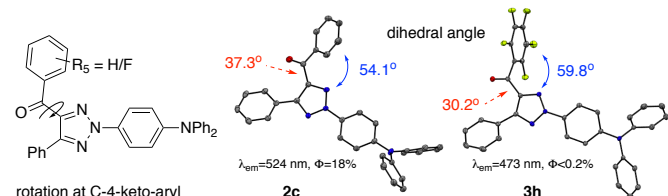


Figure 3. Crystal structures revealing large dihedral angle.

In 2001, Tang's group first introduced the concept of aggregation-induced emission (AIE) into the community.¹⁰ Since then, a great number of organic molecules have been reported with AIE properties and applied in a wide range of material research and industrial applications.¹¹ To explore the potential aggregation induced emission of these new type of fluorophores, we first measured their solid-state luminescence property. The data of some representative compounds are summarized in **Table 2** (see detailed data in Figure S19-24).

Table 2. Solid state Optical properties of EDG/EWG modified NATs

Comp	λ_{ex} (nm)	λ_{em} (nm)	Life time		Φ (%)	$\Phi_{\text{PL(solid)}}$ / $\Phi_{\text{PL(solution)}}$
			τ_{avg} (ns)			
1a	319	362	2.320		7.5	-
1b	275	372	5.426		7.5	-
1c	373	417	7.127		7.7	-
1d	363	423	1.707		30	0.38
2a	275	461	3.182		44	0.51
2b	273	457	2.224		38	0.41
2c	275	457	1.576		21	1.2
2d	274	439	2.000		51	0.53
3a	392	485	-		0.79	-
3b	390	468	2.116		9.1	15
3c	370	504	1.464		5.0	1.2
3d	417	458	-		0.73	-
3e	275	464	1.918		43	1.7
3f	368	513	4.490		13	1.1
3g	360	478	2.166		21	2.0
3h	366	481	4.507		29	161
3i	369	506	4.607		10	0.56
3j	370	502	2.662		18	0.35
3k	368	488	3.696		15	0.42
3l	368	506	2.848		8.5	2.0
3m	370	461	3.128		29	5.1
3n	370	509	5.005		7.4	0.95

Most of the EDG/EWG modified NATs exhibited solid-state emission with different wavelengths. Detailed spectroscopic data along with CIE 1931 chromaticity diagram are provided in supporting information (Figure S25). Importantly, N, N-diphenyl substitutions on N-2 aryl position is crucial for high solid-state luminance emission (such as **1d**, **2a-2c**, **3e-3n**) with quantum yields up to 40%. To understand this phenomenon, fluorescence lifetime (τ) of these NATs were measured both in solution and in the solid state. Based on those dates, radiative transition rate constants k_r and nonradiative transition rate constants k_{nr} were calculated. For compound **3h**, in THF solution, transition rate constants are $k_r=5.627 \times 10^5 \text{ s}^{-1}$ and $k_{nr}=3.128 \times 10^8 \text{ s}^{-1}$. In solid state, these rate constants are

$k_r=6.392 \times 10^7 \text{ s}^{-1}$ and $k_{nr}=1.579 \times 10^8 \text{ s}^{-1}$. Thus, it is clear that for compound **3h**, the nonradiative decay is the key factors for the low Φ_{PL} in THF solution.¹² This also lead to the observed 160 times increase of quantum yield in solid state.

By comparing the fluorescence quantum yields of these compounds in solution and solid state, we estimated that many of these new NATs might show effective AIE property, especially for those compounds with $\Phi_{\text{PL(solid)}}/\Phi_{\text{PL(solution)}} > 1$, including **2c**, **3b**, **3c**, **3e-3h**, **3l** and **3m**. In fact, the fluorescence intensity of many of these compounds decreased gradually with the increase of water content up to 70% (**Figure 4A**). This may be due to the influence of the polarity of the solvent on the TICT state.¹³ Further increase of the water fraction led to the significant increase of fluorescence intensity, reflecting typical AIE phenomenon. The titration spectra of compound **3h** are shown in **Figure 4**. (see others in Fig. S26-46). Changing the NAT sample measuring temperature from 0 to 50 °C gives a slight blue-shift in most cases, suggesting temperature has a small influence on the TICT state (Figure S13-18). Interestingly, in most of cases, addition of water (AIE test) gave unusual hypochromic shift. This may be ascribed for different emission modes of these compounds (eg. local emission vs ICT emission). This was supported by the case of **3c** where two emission bands were observed (Fig. S35). One band at short wavelength may come from the local emission while the another band is related to ICT emission. The observed hypochromic shift may be ascribed to one of these specific emission modes.

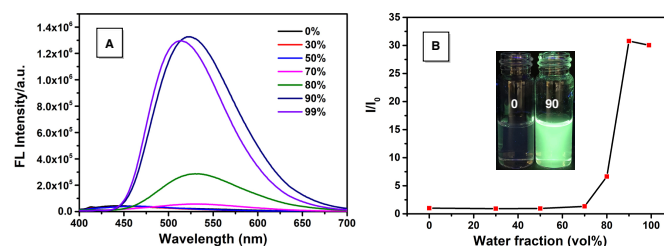


Figure 4. (A) PL spectra of **3h** (10 μM) in acetone and THF/water mixtures with different water fractions (fw). (B) Plots of emission intensity of **3h** versus the water mixtures.

During the exploration of NAT solid-state emissions, we found that some the NATs showed the mechanochromic property. Upon grinding of solid powder, some NATs showed clear red-shift emission. The emission shifts of these compounds are summarized in **Table 3**.

Table 3. NAT mechanochromic emission^[a]

	$\lambda_{\text{em-solution}}$ (nm)	$\lambda_{\text{em-solid}}$ (nm)	$\lambda_{\text{em grinding}}$ (nm)	$\Delta\lambda_{\text{em}}$ (nm)
2c	524	457	492	35
3c	550	504	514	10
3e	524	464	487	23
3g	542	478	499	21
3m	520	461	494	33

^[a]Here we discuss compounds whose fluorescence emission peaks change more than 10 nm before and after grinding.

It is known that grinding could cause the collapse of crystal lattice, converting crystalline material into amorphous material.¹⁴ This has been confirmed by the power diffraction XRD (Figure S68-72). Breaking the packing can disrupt the

intermolecular interaction, which would force the NATs to adopt a more planar conformation and contribute to the observed mechanochromic luminescence.¹⁵ This emission shift is fully reversible: heating the solid sample to 170 °C for 1 minute gave the initial emission profile with no change. This process has been repeated multiple cycles as shown in **Figure 5**. Compounds with twisted conformation (**2c**, **3c**, **3e** and **3g**) demonstrated reasonable emission change after grinding. For **3j** which have a coplanar conformation, emission in solid state did not change after grinding, suggesting that the twisted conformation between triazole (TA) and 4-arylcarbonyl may be vital to this mechanochromic luminescence. Compound **3f** and **3h**, both having twisted conformation in single crystal form (see Figure S78-86), did not show mechanochromic property. This is likely associated with the stronger steric hindrance, causing the higher energy barrier to adopt coplanar conformation. The absorption spectra of these NATs under heating and ground conditions were also measured, and there was no significant changes observed (Figure S73-77). Further mechanism studies on those phenomena are currently undergoing in our lab.

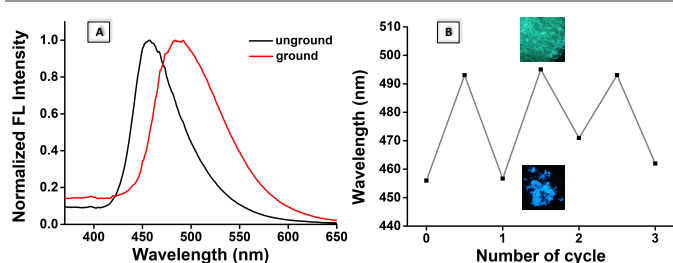


Figure 5. (A) PL spectra of unground and ground **2c**. (B) Reversible switching of the emission of **2c** through repeated grinding/heating cycles.

In summary, we reported the successful development of EDG/EWG modified NATs as a new class of organic solid fluorophores with tunable emission from blue to yellow light region. With the conformations confirmed by single crystal structures, we systematically investigated the relationship between their optical properties and their structures. Notably, the use of C-4-phenylcarbonyl group and C-5-Phenyl in triazole ring successfully led to twisted conformation which is crucial for good emission efficiency of those in solid state. What's more, some NATs revealed AIE properties and reversible mechanochromic luminescence properties, suggesting promising future for employing this strategy to prepare new organic solid fluorescent materials.

We are grateful to the NSF (CHE-1619590), NIH (1R01GM120240-01), NSFC (21228204), Jilin Province (20170307024YY, 20190201080JC) for financial support.

Conflicts of interest

There are no conflicts to declare.

Notes and references

- (a) X. Ai, Y. Chen, Y. Feng and F. Li, *Angew. Chem. Int. Ed.*, 2018, **57**, 2869-2873; (b) S. Xu, T. Liu, Y. Mu, Y. F. Wang, Z. Chi, C. C. Lo, S. Liu, Y. Zhang, A. Lien and J. Xu, *Angew. Chem. Int. Ed.*, 2015, **54**, 874-878; (c) R. Furue, T. Nishimoto, I. S. Park, J. Lee and T. Yasuda, *Angew. Chem. Int. Ed.*, 2016, **55**, 7171-7175.; (d) B. Li, J. Lan, D. Wu and J. You, *Angew. Chem. Int. Ed.*, 2015, **54**, 14008-14012; (e) H. Wang, P. Chen, Z. Wu, J. Zhao, J. Sun and R. Lu, *Angew. Chem. Int. Ed.*, 2017, **56**, 9463-9467.

- (a) J. Qi, C. Sun, A. Zebibula, H. Zhang, R. T. K. Kwok, X. Zhao, W. Xi, J. W. Y. Lam, J. Qian and B. Z. Tang, *Adv. Mater.*, 2018, **30**, e1706856; (b) J. Shi, Y. Li, Q. Li and Z. Li, *ACS Appl. Mater. Interfaces*, 2018, **10**, 12278-12294; (c) J. Mei, Y. Huang and H. Tian, *ACS Appl. Mater. Interfaces*, 2018, **10**, 12217-12261; (d) J. Qian and B. Z. Tang, *Chem.*, 2017, **3**, 56-91.
- (a) L. Yu, Z. Wu, G. Xie, W. Zeng, D. Ma and C. Yang, *Chem. Sci.*, 2018, **9**, 1385-1391; (b) M. Gao, H. Su, Y. Lin, X. Ling, S. Li, A. Qin and B. Z. Tang, *Chem. Sci.*, 2017, **8**, 1763-1768; (c) T. Yu, D. Ou, Z. Yang, Q. Huang, Z. Mao, J. Chen, Y. Zhang, S. Liu, J. Xu, M. R. Bryce and Z. Chi, *Chem. Sci.*, 2017, **8**, 1163-1168; (d) S. Dalapati, E. Jin, M. Addicoat, T. Heine and D. Jiang, *J. Am. Chem. Soc.*, 2016, **138**, 5797-5800.
- (a) J. N. Zhang, H. Kang, N. Li, S. M. Zhou, H. M. Sun, S. W. Yin, N. Zhao and B. Z. Tang, *Chem. Sci.*, 2017, **8**, 577-582; (b) S. P. Anthony, *Chem. Plus. Chem.*, 2012, **77**, 518-531.
- (a) Y. W. Zhang, X. H. Ye, J. L. Petersen, M. Y. Li and X. D. Shi, *J. Org. Chem.*, 2015, **80**, 3664-3669; (b) S. Sengupta, H. F. Duan, W. B. Lu, J. L. Petersen and X. D. Shi, *Org. Lett.*, 2008, **10**, 1493-1496; (c) Y. F. Chen, Y. X. Liu, J. L. Petersen and X. D. Shi, *Chem. Commun.*, 2008, 3254-3256; (d) Y. X. Liu, W. M. Yan, Y. F. Chen, J. L. Petersen and X. D. Shi, *Org. Lett.*, 2008, **10**, 5389-5392; (e) D. W. Wang, X. H. Ye and X. D. Shi, *Org. Lett.*, 2010, **12**, 2088-2091; (f) R. Cai, X. H. Ye, Q. Sun, Q. Q. He, Y. He, S. Q. Ma and X. D. Shi, *ACS Catalysis*, 2017, **7**, 1087-1092.
- W. M. Yan, Q. Y. Wang, Q. Lin, M. Y. Li, J. L. Petersen and X. D. Shi, *Chem. Eur. J.*, 2011, **17**, 5011-5018.
- D. Dang, Z. Qiu, T. Han, Y. Liu, M. Chen, R. T. K. Kwok, J. W. Y. Lam and B. Z. Tang, *Adv. Funct. Mater.*, 2018, **28**, 1707210.
- (a) Y. Chen, W. Zhang, Y. Cai, R. T. K. Kwok, Y. Hu, J. W. Y. Lam, X. Gu, Z. He, Z. Zhao, X. Zheng, B. Chen, C. Gui and B. Z. Tang, *Chem. Sci.*, 2017, **8**, 2047-2055; (b) Z. Li, Y. F. Wang, C. Zeng, L. Hu and X. J. Liang, *Anal. Chem.*, 2018, **90**, 3666-3669.
- Jabłoński A, *Nature*, 1933, **131**, 839-840.
- Y. Hong, J. W. Y. Lam and B. Z. Tang, *Chem. Soc. Rev.*, 2011, **40**, 5361-5388.
- (a) M. H. Lee, A. Sharma, M. J. Chang, J. Lee, S. Son, J. L. Sessler, C. Kang and J. S. Kim, *Chem. Soc. Rev.*, 2018, **47**, 28-52; (b) Z. Ruan, Y. Shan, Y. Gong, C. Wang, F. Ye, Y. Qiu, Z. Liang and Z. Li, *J. Mater. Chem. C*, 2018, **6**, 773-780; (c) R. T. Kwok, C. W. Leung, J. W. Lam and B. Z. Tang, *Chem. Soc. Rev.*, 2015, **44**, 4228-4238.
- (a) H. T. Feng, Y. X. Yuan, J. B. Xiong, Y. S. Zheng and B. Z. Tang, *Chem. Soc. Rev.*, 2018, **47**, 7452-7476.; (b) J. B. Xiong, Y. X. Yuan, L. Wang, J. P. Sun, W. G. Qiao, H. C. Zhang, M. Duan, H. Han, S. Zhang and Y. S. Zheng, *Org. Lett.*, 2018, **20**, 373-376.
- (a) M. Jiang, X. Gu, J. W. Y. Lam, Y. Zhang, R. T. K. Kwok, K. S. Wong and B. Z. Tang, *Chem. Sci.*, 2017, **8**, 5440-5446; (b) H. Sun, X.-X. Tang, B.-X. Miao, Y. Yang and Z. Ni, *Sensor. Actuat. B Chem.*, 2018, **267**, 448-456.
- (a) Y. Lei, Y. Zhou, L. Qian, Y. Wang, M. Liu, X. Huang, G. Wu, H. Wu, J. Ding and Y. Cheng, *J. Mater. Chem. C*, 2017, **5**, 5183-5192; (b) H. J. Kim, D. R. Whang, J. Gierschner, C. H. Lee and S. Y. Park, *Angew. Chem. Int. Ed.*, 2015, **54**, 4330-4333; (c) Y. Sagara, A. Lavrenova, A. Crochet, Y. C. Simon, K. M. Fromm and C. Weder, *Chemistry*, 2016, **22**, 4374-4378; (d) Z. Xie, T. Yu, J. Chen, E. Ubba, L. Wang, Z. Mao, T. Su, Y. Zhang, M. P. Aldred and Z. Chi, *Chem. Sci.*, 2018, **9**, 5787-5794.
- W. Z. Yuan, Y. Tan, Y. Gong, P. Lu, J. W. Lam, X. Y. Shen, C. Feng, H. H. Sung, Y. Lu, I. D. Williams, J. Z. Sun, Y. Zhang and B. Z. Tang, *Adv. Mater.*, 2013, **25**, 2837-2843.